Doping of Ce in T-La_2CuO_4: Rigorous test for electron-hole symmetry for high-T_c superconductivity

A. Tsukada,[1,2] H. Yamamoto,[3] and M. Naito[1]
[1]*Department of Applied Physics, Tokyo University of Agriculture and Technology, 2-24-16 Naka-cho, Koganei, Tokyo 184-8588, Japan*
[2]*NTT Basic Research Laboratories, NTT Corporation, 3-1 Morinosato-Wakamiya, Atsugi, Kanagawa 243-0198, Japan*
[3]*NTT Science and Core Technology Laboratory Group, NTT Corporation, 3-1 Morinosato-Wakamiya, Atsugi, Kanagawa 243-0198, Japan*
(Received 9 February 2006; revised manuscript received 23 June 2006; published 20 November 2006)

We report that Ce doping was achieved in La_2CuO_4 with the K_2NiF_4 (T) structure for the first time by molecular beam epitaxy. A synthesis temperature of as low as ~ 630 °C and an appropriate substrate choice, *i.e.*, (001)$LaSrGaO_4$ (a_s=3.843 Å), enabled us to incorporate Ce into the K_2NiF_4 lattice and to obtain Ce-doped T-$La_{2-x}Ce_xCuO_4$ up to $x \sim 0.06$. The doping of Ce makes T-La_2CuO_4 more insulating, which is in sharp contrast to Sr (or Ba) doping in T-La_2CuO_4, which makes the compound metallic and superconducting. The observed smooth increase in resistivity from the hole-doped side (T-$La_{2-x}Sr_xCuO_4$) to the electron-doped side (T-$La_{2-x}Ce_xCuO_4$) indicates that the electron-hole symmetry is broken in the T-phase materials.

DOI: 10.1103/PhysRevB.74.174515 PACS number(s): 74.25.Dw, 74.25.Fy, 74.72.−h, 74.72.Dn

I. INTRODUCTION

The playground for high-T_c superconductivity is the CuO_2 plane common to both p- and n-type high-T_c superconductivity, and the electronic phase diagram of high-T_c cuprates is roughly symmetric between p- and n-type doping.[1] Hence, it has been claimed that "electron-hole" symmetry holds for high-T_c superconductivity. Based on this claim, the doped Mott insulator scenario has been widely accepted,[2] in which the parent material is a Mott insulator (antiferromagnetic insulator) and high-T_c superconductivity develops when the insulator is exposed to either p- or n-type doping. However, it should be borne in mind that electron-hole symmetry is far from obvious and even surprising. Since the mother compounds of high-T_c superconductors can be regarded as charge-transfer insulators, doped holes go on the oxygen sites but doped electrons go on the copper sites, which should result in doped carriers with quite different natures. Furthermore it must be emphasized that the argument for the above "electron-hole" symmetry is based on a comparison of p- and n-type doping in different structures, namely, hole doping in the K_2NiF_4 (T) structure [*e.g.*, $La_{2-x}Sr_xCuO_4$ (LSCO)][3] and electron doping in the Nd_2CuO_4 (T') structure (*e.g.*, $Nd_{2-x}Ce_xCuO_4$).[4]

In principle, it is desirable to compare hole and electron doping in the same crystal structure, especially if one bears in mind the fact that two-types of end-member La_2CuO_4 (LCO) with the T and T' structures show quite different behavior: highly insulating T-LCO versus weakly metallic T'-LCO.[5] However, such a comparison has not yet been undertaken because it is empirically known in bulk synthesis that hole doping is possible only in octahedral (CuO_6) or pyramidal (CuO_5) cuprates, whereas electron doping is possible only in square-planar (CuO_4) cuprates. For example, electron doping in the T structure or hole doping in the T' structure has never been achieved in bulk synthesis. However, in this article we report that Ce can be incorporated into the T lattice (T-LCO) by employing a low-temperature synthetic route with molecular beam epitaxy (MBE), as evident from a monotonic change in the c-axis lattice constant. The solubility limit of Ce in the T lattice depends on the substrate material, and can be extended up to $x \sim 0.06$ with (001)$LaSrGaO_4$ (LSGO). This made it possible to perform a rigorous test on the "electron-hole" symmetry in the T-structured compounds. The result revealed that Ce doping makes T-LCO more insulating, which is in sharp contrast to Sr (or Ba) doping in T-LCO, which makes the compound metallic and superconducting. The observed smooth increase in resistivity from the hole-doped side (T-LSCO) to the electron-doped side [T-$La_{2-x}Ce_xCuO_4$ (LCCO)] indicates that the electron-hole symmetry is broken in the T-phase materials.

II. EXPERIMENT

T-LCCO thin films were grown in a custom-designed MBE chamber (base pressure $\sim 10^{-9}$ Torr) from metal sources using multiple electron-gun evaporators with atomic oxygen (1 sccm) activated by a rf power of 300 W. The details of our MBE growth process are described elsewhere.[6] There are two problems specific to the growth of T-LCCO films. The first is that Ce tends to segregate out from the T lattice at growth temperatures (T_s) higher than 700 °C.[7] Films grown at $T_s > 700$ °C showed no change in the c-axis lattice constant even when the amount of Ce was changed, indicating that Ce is not incorporated into the lattice. This problem forced us to lower the growth temperature to well below 700 °C, which led to the second problem, namely, the inclusion of T'-LCCO as an impurity phase. At low synthesis temperatures, the T' phase is easy to form and even predominates in the preparation of LCCO films even for x values as small as 0.05.[8,9] T'-LCCO is three to six orders of magnitude more conductive than T-LCCO and even exhibits superconductivity. Therefore, just a tiny inclusion of T' materials ruins the generic transport properties of the T-phase materials. As a trade-off between the first and second factors, we employed T_s=630 °C.

Epitaxial stabilization is another way to overcome the above competing problems. As we demonstrated in a previ-

 ©2006 The American Physical Society

TABLE I. The a-axis lattice constants (a_s) for the substrates used in this work.

Substrate	Abbreviation	a_s (Å)	Crystal structure
$KTaO_3$	KTO	3.989	Perovskite
$SrTiO_3$	STO	3.905	Perovskite
$LaSrGaO_4$	LSGO	3.843	K_2NiF_4
$LaAlO_3$	LAO	3.793	Perovskite
$LaSrAlO_4$	LSAO	3.755	K_2NiF_4
$PrSrAlO_4$	PSAO	3.727	K_2NiF_4
$YAlO_3$	YAO	3.715	Perovskite
$NdSrAlO_4$	NSAO	3.712	K_2NiF_4
$NdCaAlO_4$	NCAO	3.688	K_2NiF_4

ous work on the phase control of undoped LCO,[5] substrate materials have a strong influence on the selective stabilization of the T versus T' structure. Table I lists the substrate materials used in the present work. Our previous results indicated that the in-plane lattice constant (a_s) and the crystal structures of the substrate materials are crucial with regard to selective phase stabilization: substrates with a_s close to 3.80 Å and with the K_2NiF_4 structure have a strong tendency toward T-phase stabilization.[5] Utilizing epitaxial stabilization, we attempted to maximize the solubility limit of Ce in T-LCO. The typical film thickness was designed to be only 450 Å in order to make full use of the epitaxial stabilization.

After growth, most films were cooled to ambient temperature in a vacuum with P_{O2} of less than 10^{-8} Torr to avoid the introduction of excess oxygen into the films. For comparison, some films were cooled in an ozone atmosphere of P_{O3} at 10^{-5} Torr to introduce excess oxygen into the films. The films were characterized by x-ray diffraction (XRD) and resistivity measurements. All the Ce-doped T-phase films had a very high resistance (typically >100 MΩ) even at 300 K, so electrodes with a low contact resistance were required for reliable measurements. We formed the electrodes by Ag evaporation. The sampling time for the resistivity measurements also had to be set at several seconds. The valence state of Ce was determined by x-ray photoelectron spectroscopy (XPS) measurements, in which the films were transferred to a surface analysis chamber in a vacuum via a gate valve.

III. RESULTS AND DISCUSSION

A. Ce doping in the T lattice

Figure 1 shows the XRD patterns of LCCO films grown on $LaAlO_3$ (LAO) substrates with different Ce concentrations (x). The XRD patterns indicate that the films are c-axis oriented. Since the c-axis lattice constants (c_0^f) of T- and T'-LCCO are clearly different, the phase identification is rather straightforward.[5] The calculated XRD patterns are also included in Fig. 1 for reference. The films on the LAO substrates are single-phase T for $x \leq 0.045$ and single-phase T' for $x \geq 0.105$. The films are a two-phase mixture of T and T' for $x=0.06-0.09$ with T more dominant for smaller x values.[10] Figure 2 plots the c_0^f-vs-x data. The solid and open

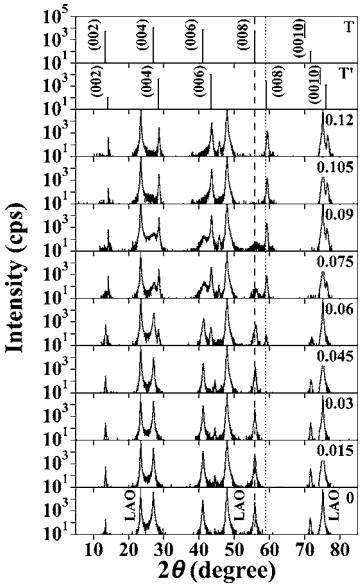

FIG. 1. X-ray diffraction patterns of $La_{2-x}Ce_xCuO_4$ films grown on $LaAlO_3$ (LAO) substrates with different Ce concentration x. The top two patterns are simulations for T- and T'-La_2CuO_4. The broken and dotted lines indicate the positions of the 008 diffraction peaks for T- and T'-La_2CuO_4, respectively. Peak positions of LAO substrates are indicated in the lowest figure.

symbols indicate T-LCCO and T'-LCCO, respectively. In the two-phase mixture region, the c_0^f values for both T- and T'-LCCO are plotted. We observe a substantial monotonic shrinkage of c_0^f with x, irrespective of T- or T'-LCCO, which confirms that Ce is actually incorporated into both the T and T' lattices under our film growth conditions.

Figure 3 provides the corresponding resistivity-vs-x plots, which show the resistivity value at 300 K [$\rho_{(300\ K)}$] as a function of Ce concentration for films grown on LAO substrates. The figure plots the data from both of the films cooled in a vacuum and those cooled in ozone. The former are denoted as "stoichiometric" since the vacuum-cooled films are almost completely oxygen-stoichiometric with presumably no excess oxygen,[11] whereas the latter are denoted as "oxidized" since ozone-cooled films have a fair amount of interstitial excess oxygen.[12] For the stoichiometric films, the

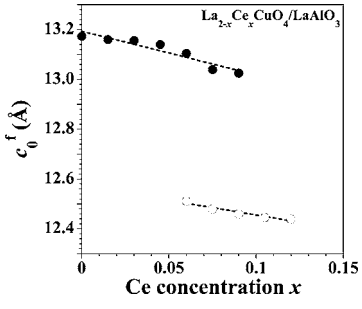

FIG. 2. Variation in the c-axis lattice constant (c_0^f) as a function of Ce concentration (x) for $La_{2-x}Ce_xCuO_4$ (LCCO) thin films grown on $LaAlO_3$ substrates. The filled and open circles indicate T- and T'-LCCO films, respectively. The dotted lines are a guide for the eye.

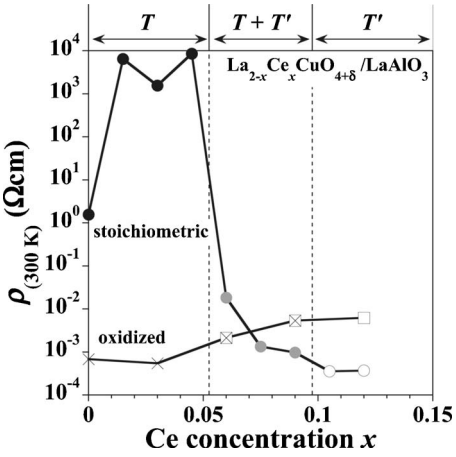

FIG. 3. Plot of the resistivity at 300 K $[\rho_{(300\ \mathrm{K})}]$ for $La_{2-x}Ce_xCuO_{4+\delta}$ films grown on $LaAlO_3$ substrates with various Ce concentrations (x). The filled, open, and gray circles indicate stoichiometric films ($\delta \sim 0$) with a single-phase T, single-phase T', and a mixed phase of T and T', respectively. The crosses, squares, and crosses with squares indicate oxidized films ($\delta > 0$) with a single-phase T, single-phase T', and a mixed T and T' phase, respectively. Each phase regime is indicated at the top of the figure.

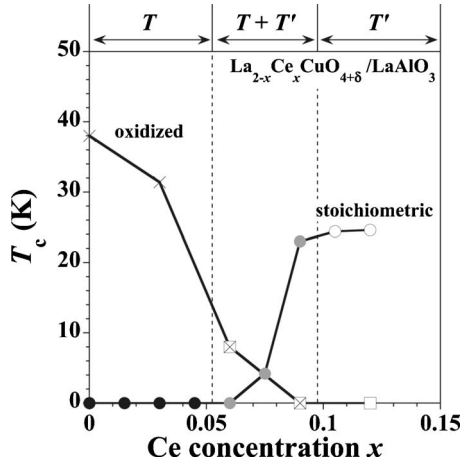

FIG. 4. Ce concentration (x) dependence of T_c for $La_{2-x}Ce_xCuO_{4+\delta}$ films grown on $LaAlO_3$ substrates. The filled, open, and gray circles indicate stoichiometric films ($\delta \sim 0$) with a single-phase T, single-phase T', and a mixed T and T' phase, respectively. The crosses, squares, and crosses with squares indicate oxidized films ($\delta > 0$) with a single-phase T, single-phase T', and a mixed T and T' phase, respectively. Each phase regime is indicated at the top of the figure.

Ce doping increases $\rho_{(300\ \mathrm{K})}$ significantly in the single-phase T region ($x \leq 0.045$). The Ce-doped films are highly insulating ($\sim 10^4\ \Omega$ cm), and their $\rho_{(300\ \mathrm{K})}$ value is three to four orders of magnitude higher than that of pristine T-LCO. It should be noted that $\sim 10^4\ \Omega$ cm is the upper limit of our resistivity measurements on 450 Å thick films, so the actual resistivity may be higher. Further Ce doping results in a slight inclusion of T'-phase materials, which greatly reduces $\rho_{(300\ \mathrm{K})}$ to $10^{-2} \sim 10^{-3}\ \Omega$ cm. In the single-phase T' region ($x \geq 0.105$), $\rho_{(300\ \mathrm{K})}$ falls to $2-3 \times 10^{-4}\ \Omega$ cm. On the oxidized films, the introduction of excess oxygen has a totally opposite effect on the T and T' phases. Excess oxygen lowers the $\rho_{(300\ \mathrm{K})}$ value of the T films by four to seven orders of magnitude, whereas it increases that of the T' films.

Figure 4 shows the superconducting transition temperature (T_c) of LCCO films as a function of Ce concentration for both stoichiometric and oxidized films grown on LAO substrates. Stoichiometric films with the T structure are highly insulating and, unsurprisingly, not superconducting. The superconductivity appears only after the introduction of excess oxygen. The T_c of oxidized T-LCCO films depends substantially on x, which is additional evidence supporting the notion that Ce is incorporated in the T lattice. If Ce were *not* in the T lattice, T_c *would* be constant. The superconductivity observed in stoichiometric films at $x \geq 0.075$ is due to the coexisting T'-phase materials.[8,9]

B. Valence of Ce

Next we discuss the valence state of Ce dopant in the T-phase materials. It is known that Ce can be trivalent as well as tetravalent. If Ce *were* trivalent, it would not be surprising for T-LCCO to be insulating. It is difficult to evaluate the Ce valence of thin films by wet chemical analysis, so it was performed by *in-situ* XPS. Figure 5 shows the Ce 3d XP spectrum of T-$La_{1.94}Ce_{0.06}CuO_4$ film [Fig. 5(a)], together with previously reported reference spectra that are representative of the Ce^{4+} and Ce^{3+} states [Fig. 5(b) and 5(c)].[13] As shown in the reference spectra, the Ce 3d spectra are characterized by complex features that are related to the final state occupation of the Ce 4f level. The assignment of each peak structure is not always well established, but the consensus is that the highest binding energy peaks (U‴ and V‴) in spectrum (b) result from a $Ce3d^94f^0O2p^6$ final state, which

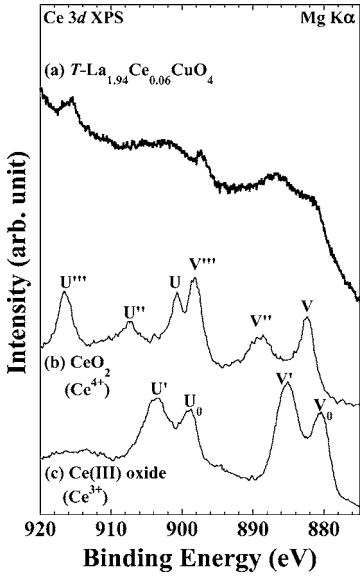

FIG. 5. (a) *In-situ* Ce 3d XP spectrum of T-$La_{1.94}Ce_{0.06}CuO_4$ thin film. Spectra (b) $CeO_2(Ce^{4+})$ and (c) Ce(III) oxide (Ce^{3+}) are for comparison (Ref. 13). Peaks U, U″, and U‴ originate from Ce $3d_{3/2}$, whereas peaks V, V″, and V‴ originate from Ce $3d_{5/2}$.

means this peak can be used as a hallmark of the tetravalent state.[13,14] The resolution of spectrum (a) is poor with a rather high background, which can be attributed to the low Ce concentration (about 0.86 at. %) and, more importantly, the charging effect due to the highly insulating state of T-$La_{1.94}Ce_{0.06}CuO_4$.[15] However, the spectrum shows distinct peaks at around 898 eV (V‴) and 916 eV (U‴), indicating that the valence of Ce in the T phase is close to +4, as in the T' phase. This conclusion is also consistent with the doping dependence of c_0^f and by the doping dependence of T_c in the oxidized films. As seen in Fig. 2, the slope of the c_0^f–x plot is almost identical in T- and T'-LCCO,[16] indicating that the ionic radius (r_i) of Ce in both compounds is close to $r_i(Ce^{4+})$ [$r_i(Ce^{4+})$=0.97 Å for coordination number (CN)=8 or 1.01 Å for CN=9] rather than $r_i(Ce^{3+})$ [$r_i(Ce^{3+})$=1.143 Å for CN = 8 or 1.196 Å for CN = 9].[17] The valence of Ce is also estimated using a method proposed by Huang *et al.*[18] The estimated valence of Ce in T- and T'-LCCO are +4.01±0.02 and +3.78±0.04, respectively. If the valence of Ce were +3, the c_0^f would be almost flat because of only a slight difference in r_i between Ce^{3+} and La^{3+} [r_i (La^{3+}) =1.160 Å for CN=8 or 1.216 Å for CN=9].

Next we may have to discuss where extra electrons added by Ce doping go: Do they remain in the $(La,Ce)_2O_2$ planes or are they injected to the CuO_2 planes? If the former were the case, electronic state of the La_2O_2 block layer would become partially $La^{3+}O^{2-}+e^-$, leading to metallic conductivity, as seen in the rare-earth monoxides, LaO, with the NaCl structure.[19] This apparently contradicts with the highly insulating state in T-LCCO. Hence, we resort to the latter possibility. The most convincing evidence of electron doping into the CuO_2 planes is Cu-O bond stretching. The best example demonstrating this stretching is that the in-plane lattice constant (a_0) expands with Ce doping in bulk $(Pr,Ce)_2CuO_4$ and $(Nd,Ce)_2CuO_4$. In the case of films, however, one must take account of the epitaxial strain effect, and the interpretation of the results requires special caution as we mention below (Sec. III D and III E). But we can safely say, at least, that the a_0 in T-LCCO is not a decreasing function with x, in spite of the substantially smaller ionic size of Ce^{4+} than La^{3+}. This is strong evidence for the injection of electrons to the CuO_2 planes. A further support can be seen in Fig. 6. Figure 6 compares the doping dependence of T_c between oxidized T -$La_{2-x}Ce_xCuO_{4+\delta}$ (LCCO+) and T-LSCO.[20] Both films are grown on $LaSrAlO_4$ (LSAO) substrates. As shown in Fig. 6, the T_c-vs-x for the T-LCCO+ films is similar to that for the T-LSCO films with a simple shift (~0.12–0.15), indicating that Ce substitution in the T-LCCO+ films compensates for hole doping with excess oxygen and the valence of Ce is close to 4+ rather than 3+. Hence, we conclude that electron doping to the CuO_2 planes is actually achieved with Ce doping.

Electron doping by Ce^{4+} substitution in T-LCO has two effects on the lattice. One is the shrinkage of the La_2O_2 block layer resulting from the substitution of small Ce^{4+} (1.01 Å) for large La^{3+} (1.216 Å),[17] which reduces c_0^f, as seen in Fig. 2. The other is the enlargement of the CuO_2 plane caused by filling electrons in the Cu-O$dp\sigma_{x2-y2}$ antibonding band.[21] The two effects contribute to a decrease in the crystallographic tolerance factor, leading to the structural transition from T to T'.[22]

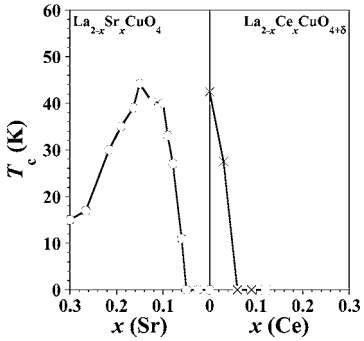

FIG. 6. Variation in T_c for $La_{2-x}Ce_xCuO_{4+\delta}$ and T-$La_{2-x}Sr_xCuO_4$ (○) (Refs. 20 and 26) as a function of Sr or Ce concentration (x). The crosses, squares, and crosses with squares indicate oxidized films ($\delta>0$) with a single-phase T, single-phase T', and a mixed T and T' phase, respectively.

C. Epitaxial stabilization of T phase

The structural transition from T to T' occurs at x =0.06–0.09 on LAO. If we are to expand the T-phase region to a higher x, the choice of substrate is important. Next we describe the epitaxial stabilization effect. Figure 7 shows the XRD patterns of LCCO films with the same x(=0.045) grown on different substrates. Caution is needed when identifying the phases of films on K_2NiF_4-type substrates, since the peak positions for the films and substrates are close to each other because of the similarity of the crystal structures.[23] In particular, the peak positions of T'-LCCO for a certain Ce concentration range become very close

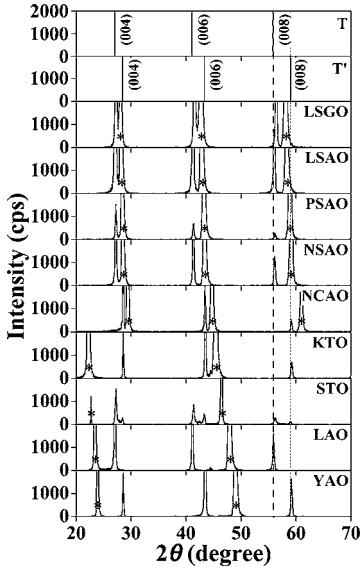

FIG. 7. X-ray diffraction patterns of $La_{2-x}Ce_xCuO_4$ films grown on various substrates with x=0.045. The top two patterns are simulations for T- and T'-La_2CuO_4. The broken and dotted lines indicate the positions of the 008 diffraction peaks for T- and T'-La_2CuO_4, respectively. Asterisks (*) indicate the substrate peaks.

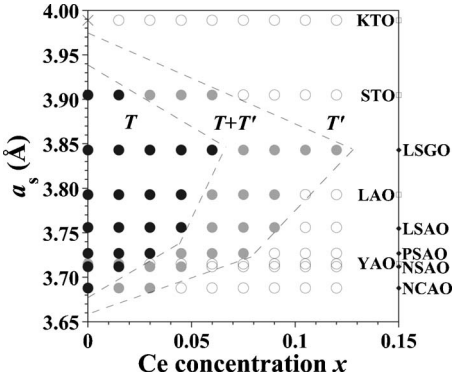

FIG. 8. Phase diagram of the selective stabilization of T versus T' in the a_s–x plane. The filled, open, and gray circles are for films with a single-phase T, single-phase T', and a mixed T and T' phase, respectively. Each region is roughly separated by broken lines. The in-plane lattice constant of each substrate is indicated on the right axis: K_2NiF_4-type (♦) and perovskite (□) substrates.

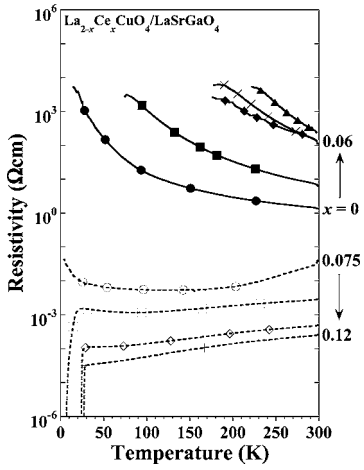

FIG. 9. Temperature dependence of resistivity for $La_{2-x}Ce_xCuO_4$ films grown on $LaSrGaO_4$ substrates with different x values. The solid lines indicate single-phase T films (●: x=0, ■: 0.015, ♦ :0.03, ▲: 0.045, ×: 0.06), while the broken line indicates mixed T- and T'-phase films (◦: 0.075, □: 0.09, ◇: 0.105, +: 0.12).

to those of the substrates. As mentioned in Fig. 3, T-LCCO is highly insulating and a slight inclusion of T'-LCCO in T-LCCO greatly reduces $\rho_{(300\ K)}$. Hence, the results of $\rho_{(300\ K)}$-vs-x plots are also taken into account to determine the phase of LCCO. It is safe to conclude that the film on LAO is single-phase T, the films on $KTaO_3$, $YAlO_3$, and $NdCaAlO_4$ (NCAO) are single-phase T', and the film on $SrTiO_3$ is a mixture of T and T'. If we judge solely from XRD results, the films on LSGO, LSAO, $PrSrAlO_4$(PSAO), and $NdSrAlO_4$ (NSAO) appear to be single-phase T. The films on LSGO and LSAO are highly insulating, so it is reasonably safe to conclude that these films are actually single-phase T. In contrast, the films on PSAO and NSAO are fairly conductive, implying the inclusion of T'-phase materials. Hence, we concluded that for PSAO and NSAO, the peaks of the T'-LCCO films are hidden by those of the substrate.

D. Phase diagram of T versus T' in a_s–x plane

Identical investigations were performed for x from 0 to 0.12 on all the substrates listed in Table I. The results are summarized in Fig. 8 as the phase diagram of T versus T' in the a_s–x plane. Approximate boundaries are also indicated in the figure, which separate single-phase T, single-phase T', and a two-phase mixture of T and T' regions. As x increases there is a transition from T to T'. The critical Ce concentration ($x_{T-T'}$) for this transition is substrate-dependent. The $x_{T-T'}$ value is maximized at 0.075–0.12 with LSGO (a_s =3.843 Å). The $x_{T-T'}$ value gradually decreases for the a_s value smaller than that of LSGO, whereas it rapidly decreases for the a_s value larger. The substrate dependence of $x_{T-T'}$ is explained by the epitaxial stabilization.[5] With no Ce doping, the in-plane lattice constant of bulk T-LCO is ~3.803 Å, so substrates with $a_s \sim 3.80$ Å such as LAO stabilize T-LCO. With Ce doping, the inherent value of the "bulk" in-plane lattice constant (a_0^b) of T-LCCO is unknown because bulk T-LCCO has not yet been synthesized. However, it should increase with increasing x because the Cu–O bond stretches with electron doping.[4,21,24] Hence, T-LCCO with a higher x value is lattice-matched with substrates that have a correspondingly larger a_s. This explains qualitatively why $x_{T-T'}$ gradually increases with increasing a_s for $a_s \leq 3.843$ Å (LSGO).[25] A further increase in a_s results in gradually better matching with T'-LCCO ($a_0^b \sim 4.01$ Å) rather than T-LCCO, which explains the rapid drop of $x_{T-T'}$ from LSGO to KTO (a_s=3.989 Å) via STO (a_s=3.905 Å).

Figure 9 shows the temperature dependence of the resistivity for films grown on LSGO substrates with different x values. As seen again in the figure, the T-LCCO films become more insulating with increasing x up to 0.06. Metallic behavior with a superconducting transition is observed in films where $x \geq 0.075$, which is due to the inclusion of T'-phase materials.[8,9]

E. Epitaxial strain

Figure 10 compares the lattice constants, a_0^f and c_0^f, of LCCO films on LSGO and LSAO substrates to illustrate the epitaxial strain effect. On an LSGO substrate, the a_0^f and c_0^f values of the film both show a rather weak dependence on x, whereas, on LSAO, a_0^f increases and c_0^f decreases monotonically with increasing x up to the T–T' phase boundary regime. The difference can be explained by taking the epitaxial strain effect into account. Although the precise values of the inherent lattice constants of "bulk" T-LCCO (a_0^b and c_0^b) are unknown as mentioned above, the relation a_s(LSAO) $< a_0^b(T\text{-LCCO}) < a_s$(LSGO) undoubtedly holds for $x \leq 0.1$. Then T-LCCO films have in-plane compressive strain on LSAO, whereas they have in-plane tensile strain on LSGO. As a result of the Poisson effect, the out-of-plane lattice constant expands on LSAO and shrinks on LSGO. Pristine T-LCO films on LSAO and LSGO are almost fully strained, with a_0^f very close to a_s. The c_0^f is 13.05 Å on LSGO and 13.22 Å on LSAO. With increasing x, a_0^b increases with electron doping, and thereby the lattice mis-

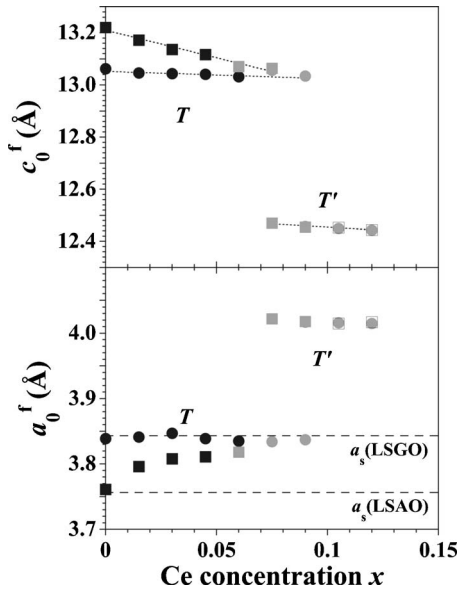

FIG. 10. Variation in the c- and a-axis lattice constant (c_0^f and a_0^f) as a function of Ce concentration (x) for $La_{2-x}Ce_xCuO_4$ thin films grown on $LaSrGaO_4$ (LSGO) and $LaSrAlO_4$ (LSAO) substrates. The circles and squares indicate films grown on LSGO and LSAO substrates, respectively. The filled, open, and gray symbols indicate films with a single-phase T, single-phase T', and a mixed T and T' phase, respectively. The dotted lines are a guide for the eye. The broken lines represent a_s=3.843 Å for LSGO and 3.755 Å for LSAO substrates.

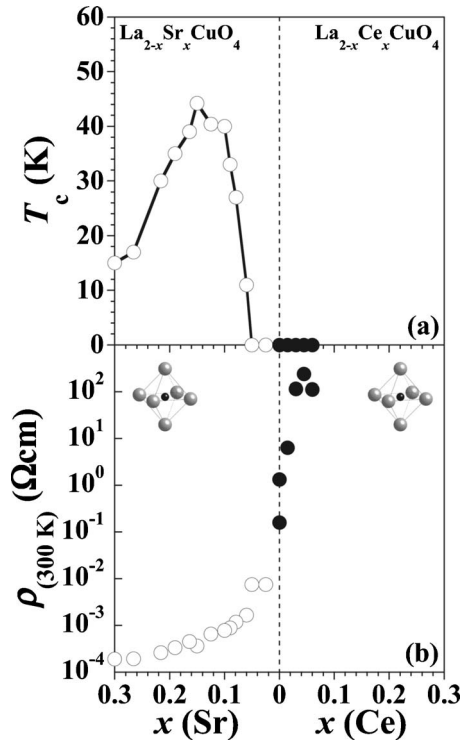

FIG. 11. Variation in (a) T_c and (b) resistivity at 300 K [$\rho_{(300\ K)}$] for T-$La_{2-x}Ce_xCuO_4$ (●) and T-$La_{2-x}Sr_xCuO_4$ (○) (Refs. 20 and 26) as a function of Sr or Ce concentration (x).

match [$\equiv(a_s-a_0^b)/a_0^b$] decreases between T-LCCO and LSGO, and increases between T-LCCO and LSAO. As seen in Fig. 10, the a_0^f of T-LCCO films on LSGO remains unchanged with doping and is almost equal to the a_s (3.843 Å) of LSGO, indicating that T-LCCO films on LSGO are fully strained for a whole range of x. In contrast, the a_0^f of T-LCCO films on LSAO increases steeply and approaches the a_0^f values on LSGO for higher x values. This indicates that T-LCCO films on LSAO are fully strained only at x=0 and become more strain-relaxed with increasing x. The different strain relaxation of the films on LSGO and LSAO is reflected also in the c_0^f-vs-x plot. The slope of c_0^f-vs-x is significantly different between T-LCCO films on LSGO and on LSAO. The slope on LSAO is much steeper than that on LSGO. There are two contributors to the change in c_0^f with increasing x, namely, the decrease due to Ce^{4+} substitution and the change in the degree of strain. On LSAO, the compressive strain relaxes more as x increases, which reduces the out-of-plane Poisson expansion, resulting in the additional decrease in c_0^f. On LSGO, the tensile strain decreases because of the better lattice match with a higher x, which reduces the out-of-plane Poisson compression, resulting in partial compensation for the c_0^f decrease due to Ce^{4+} substitution. The large epitaxial-strain effect observed in T-LCCO is hardly observed in T'-LCCO. In the T' phase, the lattice mismatch between T'-LCCO ($a_0^b \sim 4.01$ Å) and substrates (a_s=3.843 Å for LSGO and 3.756 Å for LSAO) is too large to sustain epitaxial strain.

F. Electron-hole symmetry

Figure 11 shows the "global" electronic phase diagrams from hole to electron doping in T-LCO, where (a) T_c and (b) $\rho_{(300\ K)}$ are plotted as a function of Ce or Sr concentration. The data for the electron-doped regime are taken from the present work on T-LCCO grown on LSGO, in which the electron doping is maximized up to x=0.06. The data for the hole-doped regime are taken from our previous work on T-LSCO grown on LSAO.[20,26] In T-LCO, superconductivity appears only with hole doping, although it cannot be ruled out that superconductivity might appear with electron doping beyond 0.06. More important is the behavior of $\rho_{(300\ K)}$. Electron doping and hole doping in T-LCO provide a sharp contrast. Hole doping metallizes T-LCO, whereas electron doping makes T-LCO more insulating. The $\rho_{(300\ K)}$ value starts to rise rapidly with a break in the slope of the $\rho_{(300\ K)}$-vs-x curve for hole doping of about 0.05 and steadily increases up to electron doping of about 0.06. In fact, we do not see any singularity at x=0. Figure 11 appears to show broken electron-hole symmetry in the T phase.

As mentioned in the Introduction, it has been claimed that the electron-hole symmetry appears to hold in high-T_c superconductors, but this statement is based on a comparison of hole and electron doping in different structures, namely, hole doping in the K_2NiF_4 (T) structure and electron doping in the Nd_2CuO_4 (T') structure.[3,4] It has to be emphasized that the mother compounds of the two structures, T-LCO and T'-LCO, have quite different electronic properties, as revealed by our previous work.[5] T-LCO is highly insulating,

whereas T'-LCO is fairly metallic.[27] Furthermore, a striking contrast is observed for Ce doping in T-LCO and T'-LCO; Ce doping makes T-LCO insulating, whereas it makes T'-LCO superconducting (Fig. 9). This indicates that the Cu-O coordination totally changes the electronic phase diagram of high-T_c superconductivity. Hence, it is desirable to establish a global electronic phase diagram from hole to electron doping in the same crystal structure with octahedral, pyramidal, and square-planar Cu-O coordinations. Such attempts have been made with respect to bulk synthesis but have proved unsuccessful. Our present work, however, demonstrates that a low-temperature thin-film synthesis route may enable such an exploration.

G. Nature of insulating state in *T*-LCCO

Next, we must discuss the nature of the insulating state in electron-doped T-LCO. If T-LCO were a simple Mott insulator, electron doping would lead to a metallic state, but our experimental results show just the opposite. Thus, we have to think of other possible insulating mechanisms in electron-doped T-LCO. One simple explanation is that electron doping by Ce compensates for hole doping with remnant excess oxygen, which is not removed when films are cooled in a vacuum. However, if it were the case, as much as $\delta=0.03$ excess oxygen would be required after vacuum cooling to account for the fact that T-LCCO films are still insulating with Ce doping up to $x=0.06$. This is unlikely.

Another explanation is to regard the antiferromagnetic (AF) insulating ground state in T-LCO as a Fermi-surface driven spin-density-wave (SDW) state. Then, Fermi surface nesting could occur over a larger area at finite electron doping than at zero doping, depending on the shape of the Fermi surface. However, the Fermi surface nesting is usually incomplete in two- or three-dimensional materials and leaves some pieces of the Fermi surface; hence, it may be hard to explain the highly insulating state of T-LCO and T-LCCO.

The third explanation is based on the ionic model, which describes T-LCO as a charge-transfer insulator. In this framework, doped holes go on the oxygen sites, creating spin frustration. The long-range AF order is promptly destroyed with hole doping, thereby leading to metallic conduction and superconductivity. In contrast, doped electrons go on the Cu sites, eliminating Cu spins leading to spin dilution instead of spin frustration. The AF order may not be destroyed until deep electron doping. In this AF lattice with $Cu^{2+}(S=1/2, d^9)$, even though electrons are doped, they are not easy to move. For example, an up-spin electron that comes on a down-spin Cu site is unable to hop to the nearest neighbor up-spin Cu sites as described by the Pauli principle. It can hop only to the Cu 4s level at the cost of the 3d–4s energy difference. This explanation, though appearing plausible, should create a certain singularity at $x=0$ within the pure ionic model, and totally neglects substantial hybridization between the O 2p and Cu 3d states, predominating in high-T_c cuprates.

As the final possible explanation, we should note that the insulating behavior starts at hole doping of $x\sim0.05$ and is continuous at $x=0$. So the insulating nature in the hole-doped and electron-doped regimes may have the same origin. In hole-doped T-LSCO, the low-temperature upturn in normal-state resistivity exists even at optimum doping, develops as x decreases, and rapidly grows below $x=0.05$ with the disappearance of superconductivity.[28,29] There have been certain indications that the development of the low-temperature upturn is related to the growth of the pseudogap. Although the origin of the pseudogap has not yet been elucidated,[28,30] the present results can be interpreted phenomenologically by assuming that the pseudogap in T-LCO remains robustly or even grows with electron doping, whereas it collapses with hole doping.

IV. SUMMARY

We synthesized T-$La_{2-x}Ce_xCuO_4$ with $x\leq0.06$ by molecular beam epitaxy and investigated the effect of electron doping on T-La_2CuO_4. The key to synthesizing T-$La_{2-x}Ce_xCuO_4$ with large x is the choice of lattice-matched substrate, $LaSrGaO_4$ ($a_s=3.843$ Å). All T-$La_{2-x}Ce_xCuO_4$ films were insulating and became more insulating with electron doping in the range of $x\leq0.06$. The result so far obtained indicates that the electron-hole symmetry appears to be broken in T-La_2CuO_4. Furthermore, the insulating nature in T-$La_{2-x}Ce_xCuO_4$ may be ascribed not to a simple Mott-insulator scenario but is strongly related to the development of the pseudogap in T-structure compounds. As a future work, it may be an important question to see whether superconductivity might appear with further electron doping over 0.06 or not. In order to explore the possibility to push further the electron doping limit, one candidate may be the doping of Th with a slightly larger ionic radius than Ce.

ACKNOWLEDGMENT

The authors thank S. Karimoto, H. Shibata, H. Sato, K. Ueda, T. Makimoto, T. Yamada, and A. Matsuda for helpful discussions, and K. Torimitsu, M. Morita, H. Takayanagi, and S. Ishihara for their support and encouragement throughout the course of this study.

[1] M. B. Maple, MRS Bull. **15**, 60 (1990).
[2] P. W. Anderson, *The Theory of Superconductivity in the High-T_c Cuprates* (Princeton University Press, Princeton, NJ, 1997).
[3] H. Takagi, T. Ido, S. Ishibashi, M. Uota, S. Uchida, and Y. Tokura, Phys. Rev. B **40**, 2254 (1989).
[4] Y. Tokura, H. Takagi, and S. Uchida, Nature (London) **337**, 345 (1989).
[5] A. Tsukada, T. Greibe, and M. Naito, Phys. Rev. B **66**, 184515 (2002).
[6] M. Naito, H. Sato, and H. Yamamoto, Physica C **293**, 36 (1997).

[7] E. Takayama-Muromachi, Y. Uchida, and K. Kato, Physica C **165**, 147 (1990).
[8] M. Naito and M. Hepp, Jpn. J. Appl. Phys., Part 2 **39**, L485 (2000).
[9] M. Naito, S. Karimoto, and A. Tsukada, Supercond. Sci. Technol. **15**, 1663 (2002).
[10] Small peaks at $2\theta \sim 44.4°$ and $\sim 45.8°$ are unidentified, but it should be noted that the former appear together with *T*-LCCO and the latter with *T′*-LCCO.
[11] The stoichiometric sample might have a few oxygen deficiencies in the CuO_2 plane.
[12] H. Sato, M. Naito, and H. Yamamoto, Physica C **280**, 178 (1997).
[13] D. R. Mullins, S. H. Overbury, and D. R. Huntley, Surf. Sci. **409**, 307 (1998).
[14] J. P. Holgado, G. Munuera, J. P. Espinos, and A. R. Gonzalez-Elipe, Appl. Surf. Sci. **158**, 164 (2000).
[15] Since the Ce 3*d* signal was rather weak due to the low Ce concentration in *T*-LCCO, we adopted a fairly high pass energy for the analyzer (50 eV) to obtain the spectrum in a reasonable time ($\sim$1 day) at the cost of resolution.
[16] M. Naito, A. Tsukada, T. Greibe, and H. Sato, Proc. SPIE **4811**, 140 (2002).
[17] R. D. Shannon, Acta Crystallogr. **A32**, 751 (1976).
[18] T. C. Huang, E. Moran, A. I. Nazzal, J. B. Torrance, and P. W. Wang, Physica C **159**, 625 (1989); The estimated Ce valence in *T′*-$Nd_{2-x}Ce_xCuO_4$ was +3.84, which well coincided with the value estimated by Idemoto *et al.* (+3.84) [see Physica C **166**, 513 (1990)].
[19] J. M. Leger, N. Yacoubi, and J. Loriers, J. Solid State Chem. **36**, 261 (1981).
[20] H. Sato, A. Tsukada, M. Naito, and A. Matsuda, Phys. Rev. B **61**, 12447 (2000).
[21] E. Wang, J.-M. Tarascon, L. H. Greene, G. W. Hull, and W. R. McKinnon, Phys. Rev. B **41**, 6582 (1990).
[22] J. Bringley, S. S. Trail, and B. A. Scott, J. Solid State Chem. **86**, 310 (1990).
[23] This problem does not arise with perovskite-type substrates.
[24] Thin films are strained as described in the next section, so it is very difficult to estimate the "bulk" lattice constants of *T*-LCCO.
[25] In other words, the fact that $x_{T-T'}$ is larger in LSGO than in LAO is one evidence that strongly supports electron doping in the CuO_2 planes.
[26] H. Sato, A. Tsukada, M. Naito, H. Yamamoto, and A. Matsuda, *Studies of High Temperature Superconductors*, edited by A. Narlikar (Nova Science Publishers, New York, 2000), Vol. 34, p. 203.
[27] We have recently discovered superconductivity with $T_c > 20$ K in nominally undoped *T′*-$La^{3+}_{2-x}RE^{3+}_xCuO_4$ (RE=rare-earth elements); A. Tsukada, Y. Krockenberger, M. Noda, H. Yamamoto, D. Manske, L. Alff, and M. Naito, Solid State Commun. **133**, 427 (2005).
[28] T. Sekitani, H. Sato, M. Naito, and N. Miura, Physica C **378-381**, 195 (2002).
[29] T. Sekitani, H. Sato, M. Naito, and N. Miura, Physica C **388-389**, 345 (2003).
[30] We have proposed the Kondo effect (namely, Kondo singlet formation) as the origin of the pseudogap [see T. Sekitani *et al.*, cond-mat/0301090].